

have prevented the hydrolysis of tetraglycine. Tetraglycine therefore reentered the reaction region and further reacted with a glycine, producing a diglycine, a triglycine, or a diketopiperazine molecule when the amount of tetraglycine becomes sufficient. The presence of even-numbered oligomers up to hexaglycine and the absence of detectable amounts of both tri- and pentaglycine suggest that the chain elongation proceeds mainly by aminolysis of diketopiperazine.

As monomers of biological significance, both amino acid and nucleotide molecules can potentially accommodate stepwise polymerization schemes into themselves (2, 3) [for instance, by repeating the cycle of hydrolysis and elongation (4)]. From an evolutionary perspective, a more pressing issue in this regard is how to implement such schemes. Stepwise synthesis of oligoglycine in our flow reactor seems to suggest that submarine hydrothermal vents in the Archean ocean could have readily facilitated the multiplicative oligomerization of these monomers, even in the absence of ribosomes or ribozymes.

References and Notes

1. M. Eigen, *Naturwissenschaften* **58**, 465 (1971).
2. K. Matsuno, *BioSystems* **15**, 1 (1982).
3. S. A. Kauffman, *J. Theor. Biol.* **119**, 1 (1986).
4. L. E. Orgel, *ibid.* **123**, 127 (1986).
5. T. Nakashima, J. R. Jungck, S. W. Fox, D. Lederer, B. C. Das, *Int. J. Quantum Chem. QBS4*, 65 (1977); C. Huber and G. Wächtershäuser, *Science* **281**, 670 (1998); M. Keller, E. Blöchl, G. Wächtershäuser, K. O. Stetter, *Nature* **368**, 836 (1995); A. Brack, *Origins Life Evol. Biosphere* **17**, 367 (1987); B. M. Rode and G. Schwendinger, *ibid.* **20**, 401 (1990); G. Wächtershäuser, *Prog. Biophys. Mol. Biol.* **58**, 85 (1992); J. Bujdak, K. Faybikova, A. Eder, Y. Yongyai, B. M. Rode, *Origins Life Evol. Biosphere* **25**, 431 (1995); L. E. Orgel, *ibid.* **28**, 227 (1998); J. P. Ferris, A. R. Hill Jr., R. Liu, L. E. Orgel, *Nature* **381**, 59 (1996); A. D. Keefe, G. L. Newton, S. L. Miller, *ibid.* **373**, 683 (1995); M. P. Robertson and S. L. Miller, *ibid.* **375**, 772 (1995).
6. J. B. Corliss *et al.*, *Science* **203**, 1073 (1979); J. M. Edmond, K. L. Von Damm, R. E. McDuff, C. I. Measures, *Nature* **297**, 187 (1982); H. Yanagawa and K. Kojima, *J. Biochem.* **97**, 1521 (1985); M. J. Russell, A. J. Hall, A. G. Cairns-Smith, P. S. Braterman, *Nature* **336**, 117 (1988); E. L. Shock, *Ciba Found. Symp.* **202**, 40 (1996).
7. J. P. Ferris, *Origins Life Evol. Biosphere* **22**, 109 (1992); J. P. Amend and E. L. Shock, *Science* **281**, 1659 (1998).
8. K. Matsuno, *Protobiology: Physical Basis of Biology* (CRC Press, Boca Raton, FL, 1989). When a small hot body comes into contact with a large cold body, the temperature of the hot body decreases. In particular, the actual temperature drop is the fastest possible alternative. If the slower process was to take over, the heat flow toward the cold body would increase because of the greater temperature difference between the two bodies. The greater transference of heat energy toward the cold body with a smaller temperature drop of the hot body in time is, however, a self-contradiction. Actualization of the fastest temperature drop is selective in comparison to generative thermal synthesis at a high temperature.
9. J. L. Bada, S. L. Miller, M. Zhao, *Origins Life Evol. Biosphere* **25**, 111 (1995).
10. K. Matsuno, *Viva Orig.* **25**, 191 (1997). Although there might have been a difficulty in synthesizing amino acid molecules in the environment on primitive Earth, the recent collection of micrometeorites in Antarctica suggests that extraterrestrial amino acids might have been

delivered to primitive Earth [compare F. Brinton, C. Engstrand, D. P. Glavin, J. L. Bada, M. Maurette, *Origins Life Evol. Biosphere* **28**, 413 (1998)].

11. The stirring condition was confirmed by measuring the through-time of the marker, vitamin B₁₂, in the whole closed circuit under the pressurized condition, but without heating.
12. After the reactor was operated for 1 hour, the pH of the circulating fluid increased from an initial pH

of 2.5 to a pH of 2.9, suggesting an involvement of catabolic reactions.

13. M. Nagayama, O. Takaoka, K. Inomata, Y. Yamagata, *Origins Life Evol. Biosphere* **20**, 249 (1990).
14. We thank A. Maeshima, Y. Ogata, and M. Sato for their assistance in performing the experiments reported here.

1 October 1998; accepted 23 December 1998

Oligomeric Structure of the Human EphB2 Receptor SAM Domain

Christopher D. Thanos, Kenneth E. Goodwill, James U. Bowie*

The sterile alpha motif (SAM) domain is a protein interaction module that is present in diverse signal-transducing proteins. SAM domains are known to form homo- and hetero-oligomers. The crystal structure of the SAM domain from an Eph receptor tyrosine kinase, EphB2, reveals two large interfaces. In one interface, adjacent monomers exchange amino-terminal peptides that insert into a hydrophobic groove on each neighbor. A second interface is composed of the carboxyl-terminal helix and a nearby loop. A possible oligomer, constructed from a combination of these binding modes, may provide a platform for the formation of larger protein complexes.

Proteins containing SAM domains include the Eph family of receptor tyrosine kinases (1), diacylglycerol kinases (2), serine-threonine kinases (3), Src homology 2 (SH2) domain-containing adapter proteins (4, 5), ETS transcription factors (6), polyhomeotic proteins (6, 7), and the connector enhancer of KSR (kinase suppressor of ras) (8), among others. The presence of a SAM domain in a wide variety of proteins suggests that, like other signal transduction modules (9), it confers a common function.

Previous studies suggest that SAM domains form SAM homo-oligomers and SAM hetero-oligomers. First, the SAM domain from the ETS transcription factor TEL (TEL-SAM) has been shown to self-associate (10). In many human leukemias, chromosomal translocations render the TEL-SAM domain fused to other proteins including the tyrosine kinase domains of Abelson leukemia virus kinase, platelet-derived growth factor receptor- β , and Janus kinase 2 as well as the transcription factor AML1 (11, 12). TEL-SAM domain oligomerization results in constitutive activation of the protein to which the SAM domain is fused and may cause cell transformation (13). Second, SAM domains from various polycomb group (PcG) proteins, which regulate homeotic gene transcription, also form specific homo- and hetero-

oligomers and may be important for generating large PcG protein complexes within the cell (6, 14). Third, the SAM domains of Byr2 and Ste4, proteins that regulate sporulation in the yeast *Schizosaccharomyces pombe*, form a hetero-oligomer (3, 14–16).

SAM domains also bind to proteins that do not contain SAM domains. The LAR (leukocyte common antigen related) protein tyrosine phosphatase (PTP) binds to a region of LIP (LAR-interacting protein) that consists of three tandem SAM domains, indicating that SAM domains bind directly to PTPs (17). Other evidence supports a role for SAM domains in PTP binding. Stein *et al.* reported that binding of low molecular weight PTP (LMPTP) to the EphB1 receptor tyrosine kinase is abrogated by a Y929F mutation (in which Tyr⁹²⁹ is mutated to Phe) in the SAM domain (18). This same mutation also abolished binding of the SH2-containing adapter protein Grb10 (19). These data suggest that phosphorylation of Tyr⁹²⁹ in the EphB1 receptor SAM domain creates a binding site for LMPTP and Grb10 (18). Finally, the PDZ domain of the ras-binding protein AF6 recognizes a peptide that corresponds to the COOH-terminus of the SAM domain in various Eph receptors (20).

Here we report the crystal structure of the SAM domain from the EphB2 receptor. The Eph receptors are the largest family of receptor tyrosine kinases and have been implicated in the regulation of segmentation of the developing brain, retinotectal axon guidance and bundling, angiogenesis, and cell migration (21). All Eph receptors contain a SAM domain at their COOH-terminus.

UCLA-DOE Laboratory of Structural Biology and Molecular Medicine and Department of Chemistry and Biochemistry, University of California, Los Angeles, CA 90095, USA.

*To whom correspondence should be addressed. E-mail: bowie@mbi.ucla.edu

REPORTS

A SAM domain-containing fragment of the EphB2 receptor, EphB2-SAM, corresponding to residues 905 to 981 in the full-length receptor, was expressed in *Escherichia coli*. A variant of EphB2-SAM containing selenomethionine (22) was prepared and crystallized in

space group $P4_1$ with cell dimensions $a = b = 73.90 \text{ \AA}$ and $c = 104.57 \text{ \AA}$ (23). The asymmetric unit of the crystal contained eight EphB2-SAM monomers. The structure was solved with the multiwavelength anomalous dispersion (MAD) method with data collected at four

wavelengths (Table 1) (24). The structure was refined using CNS (Crystallography and NMR System) with phase restraints at a resolution of 1.95 \AA (25). The R_{cryst} is 22.8% and the R_{free} is 27.3%.

The EphB2-SAM domain structure is shown in Fig. 1. The polypeptide chain starts with a stretch of irregular structure and enters the core of the domain beginning with helix 1 (residues 14 to 20). The chain then reverses direction into helix 2 (residues 27 to 32). A long loop then wraps around the domain and contains a single turn of helix 3 (residues 38 to 41). After the loop region, the chain enters helix 4 (residues 46 to 52), and then takes a sharp turn into the long COOH-terminal helix 5 (residues 57 to 78) (26).

The sites of known and proposed protein interactions with the SAM domain are shown in Fig. 1. The binding site of the AF6 PDZ domain is located at the end of helix 5, which extends out from the core of the structure, making the binding site readily accessible. Residue Tyr²⁶, which is a putative phosphorylation site and binding site for LMPTP and Grb10, is found at the start of helix 2 (Fig. 1A). Although Tyr²⁶ is partially buried in the structure and participates in a hydrogen bond with His⁵⁹, a phosphoryl group could be accommodated by slight rearrangements of the structure. Such conformational changes are not unprecedented (27).

Each EphB2-SAM monomer in the crystal engages in two types of interactions, which bury large amounts of surface area. The first interface type involves the exchange of NH₂-terminal peptide arms between adjacent SAM domains. This "arm-exchange" interface buries ~1900 Å² of total surface area. The dimer is asymmetric with one NH₂-terminus forming a curved structure (S-form) and the other NH₂-

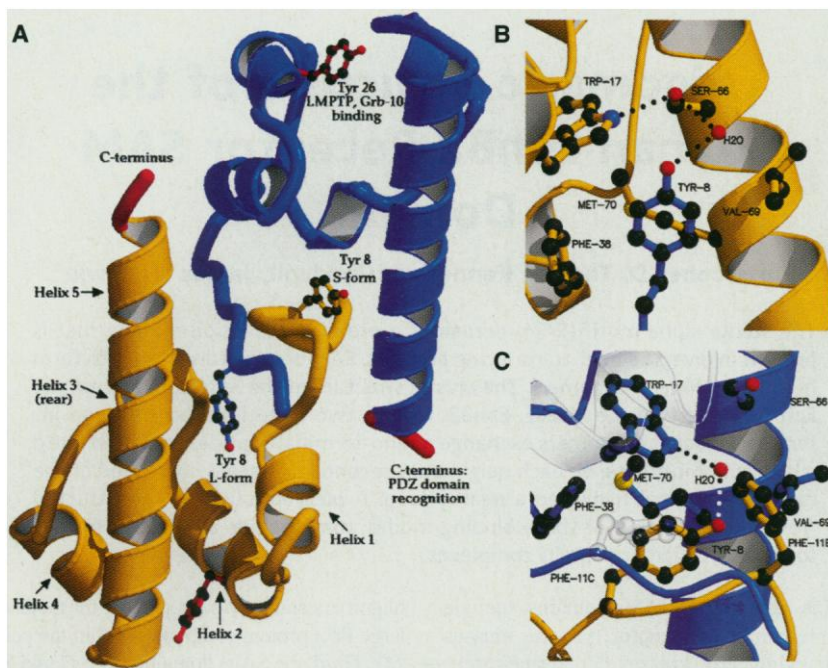


Fig. 1. The arm-exchange interface. (A) Ribbon structure of the EphB2 SAM domain. The L-form of the polypeptide is outlined in blue, the S-form is outlined in yellow, and Tyr⁸ is shown in ball and stick representation. The areas of the structure that interact with other proteins are highlighted in red. In our numbering, Tyr²⁶ corresponds to Tyr⁹²⁹ in the EphB1 receptor (23). (B) Close-up view of the L-form peptide insertion. In the L-form, Tyr⁸ packs into a hydrophobic pocket (Phe¹¹ is not shown, Phe³⁸, Met⁷⁰, Trp¹⁷, and Val⁶⁹) and hydrogen bonds through an ordered water molecule to Ser⁶⁶. (C) Close-up view of the S-form peptide insertion. In the S-form, Tyr⁸ inserts into the same pocket as in the L-form, but it hydrogen bonds to Trp¹⁷ through an ordered water molecule. Residue Phe^{11C} (L-form) and helix 1 are shown in transparent representation to better illustrate the packing around Tyr⁸ and the architecture of Trp¹⁷ in the hydrophobic patch. The figures were made with MOLSCRIPT (33).

Table 1. Crystallographic data, phasing, and refinement. Diffraction data were collected at 100 K on beamline 5.0.2 at the Advanced Light Source, Lawrence Berkeley National Laboratory. A Q4 charge-coupled device detector was used. The selenium atom positions were determined with the peak anomalous difference data in the program Shake-and-Bake v.2.0 (34). MAD phases were generated with MLPHARE (34) and solvent flattening was applied in DM (34). There were eight protein molecules in each asymmetric unit. All selenium

atoms except for the NH₂-terminal selenomethionines were located, for a total of 48 sites. The model was built with the program O (34). CNS was used for refinement (25, 34). The MLHL maximum likelihood target function was used with density-modified phases as prior experimental phase information. Restrained individual *B*-factor refinement, anisotropic *B*-factor correction, and a bulk solvent model were used in the refinement. The Protein Data Bank accession code for this protein is 1b4f.

Data set	λ (Å)	d_{MIN} (Å)	Crystallographic data				$\langle I \rangle / \langle \sigma_I \rangle$	R_{sym}^* (%)	$\langle PP \rangle^\dagger$ acen/cen
			Observed reflections	Unique reflections	Completeness (%)				
Anomalous peak	0.97966	1.95	223,269	39,547	96.5	17.6	4.7 (16.3)	1.64/0.00	
Inflection point	0.97982	1.95	168,469	38,997	95.1	17.2	4.2 (18.4)	1.24/0.00	
High-energy remote	0.96859	1.95	183,660	39,507	96.4	17.4	4.8 (24.9)	1.73/1.24	
Low-energy remote	1.00000	2.00	178,021	36,232	95.2	19.3	4.2 (19.5)	1.45/1.05	
Phasing and refinement									
Overall figure of merit to 1.95 Å			MLPHARE: 0.656		DM: 0.749				
R factor [‡]			R_{cryst} : 22.8%		R_{free} : 27.3%				
RMSD from ideality [§]			Bond lengths: 0.028 Å		Bond angles: 1.90°				
Ramachandran analysis			Most favored: 92.5%		Additionally allowed: 7.5%				

* $R_{\text{sym}} = \frac{\sum_n \sum_i |I_i(h) - \langle I(h) \rangle|}{\sum_n \langle I(h) \rangle}$, where $I_i(h)$ is the i th measurement and $\langle I(h) \rangle$ is the weighted mean of all measurements of $I(h)$ for Miller indices h . Values in parentheses are for the highest resolution bins. [†]Phasing power is the mean value of the heavy atom structure factor amplitude divided by the residual lack of closure error for both acentric

and centric reflections. [‡] R factor = $\frac{\sum |F_o - F_c|}{\sum |F_o|}$, where F_o and F_c are the observed and calculated structure factors, respectively. R_{free} is the cross-validation R factor calculated for 10% of the reflections omitted in the refinement process. [§]RMSD is the root mean square deviation.

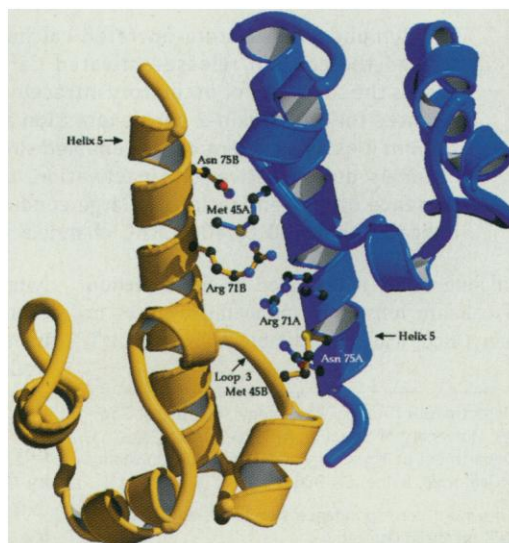
REPORTS

terminus extending more directly into its partner's binding pocket, adopting a linear shape (L-form). In both forms, the conserved hydrophobic position Tyr⁸ anchors the interface. As shown in Fig. 1, Tyr⁸ inserts into a hydrophobic cavity created by Phe¹¹, Trp¹⁷, Phe³⁸, Val⁶⁹, and Met⁷⁰ of the adjacent monomer. In the S-form, the phenolic hydroxyl forms a water-mediated hydrogen bond to the ϵ -nitrogen of the highly conserved Trp¹⁷. In the L-form, a water-mediated hydrogen bond is made to Ser⁶⁶. The position analogous to Tyr⁸ in the PcG protein *ph* is a tryptophan and, when changed to alanine, binding to other SAM domains is abolished (6). This result suggests that the arm-exchange interface may provide a general mechanism for SAM domain association.

The second type of interface buries $\sim 1250 \text{ \AA}^2$ of surface area and is formed by packing helix 5 and loop 3 (residues 42 to 45, between helices 3 and 4) of one monomer against the same elements of the other monomer with pseudodyad symmetry (see Fig. 2). Because the helix and loop of one monomer form a "b" shape, we refer to this association as the b-region interface. The residues that bury the most surface area in the interface are Met⁴⁵, Arg⁷¹, and Asn⁷⁵. Residue Met⁴⁵ protrudes out from loop 3 and packs into the side chains of Asn⁷¹ and Arg⁷⁵ from the opposite monomer. Residues Asn⁷¹ and Arg⁷⁵ form hydrogen bonds with the main chain of the adjacent subunit.

The presence of two distinct intermonomer binding surfaces suggests that SAM domains could form extended polymeric structures. An example of such a polymer, constructed from repeated combinations of arm-exchange interfaces and b-region interfaces, is shown in Fig. 3. The putative SAM domain polymer has a highly asymmetric charge distribution (Fig. 3C). One face of the oligomeric structure has a strongly negative potential, whereas the opposite face is largely neutral.

Fig. 2. The b-region interface. In this interface, Asn⁷⁵ and Arg⁷¹ form hydrogen bonds to the main chain of the opposite monomer. Methionine-45 packs against helix 5 from a neighbor. This figure was made with MOLSCRIPT (34).



Neither the monomeric SAM domain nor the two dimeric forms exhibit a notable charge distribution. However, a striking asymmetric charge distribution develops as a consequence of oligomer formation.

Several lines of evidence suggest that the putative SAM domain oligomer may be biologically significant and is not simply a result of crystallization. First, both interfaces bury more than twice the average surface area seen in crystal contacts, indicating that the interfaces were not formed by chance (28). For comparison, PDZ domain and SH2 domain peptide complexes bury between 700 and 1100 \AA^2 total surface area, respectively (29). Second, as noted above, mutation of the most deeply buried residue in the arm-exchange interface is known to disrupt oligomerization of the *ph* SAM domain (6). Thus, what we see structurally is recapitulated biochemically. Third, the polymer cannot be generated by the application of crystallographic symmetry operations alone, but instead involves three noncrystallographic symmetry operations. Thus, the polymer is not simply a necessary consequence of crystallization. Fourth, the polymer is compatible with the binding of LMPTP, AF6, and Grb10. The known and putative binding sites for these proteins are all exposed and accessible for binding. Finally, the charge distribution in the polymer is not random and is a consequence of polymerization. Moreover, most of the surface acidic residues that create the negative surface of the polymer are highly conserved in the Eph receptor family (30).

Because spontaneous SAM domain aggregation might cause constitutive kinase activation, SAM domain oligomerization in the Eph receptor family would need to be regulated in some fashion. Indeed, equilibrium sedimentation experiments reveal that the EphB2-SAM domain is monomeric at concentrations in the range of 100 μM (31). It is possible that ligand-induced receptor activation results in a confor-

mational change that facilitates SAM domain association. Alternatively, receptor aggregation could provide the driving force for SAM domain oligomerization. This mechanism is consistent with polymer formation in our crystals because only a high concentration would be required. If so, the oligomeric state of the Eph receptor SAM domains could be controlled by the aggregation state of the ligand. Stein *et al.* have shown that when Eph receptors were presented with a dimeric ligand, tyrosine kinase activity was stimulated, but many other signaling events were only triggered by tetramerized ligand (18). For example, only tetramerized ligand caused recruitment of LMPTP to the EphB2 receptor, an association that is mediated by the receptor's SAM domain (18). If aggregated ligand creates higher order SAM domain oligomers, new binding surfaces may be created that facilitate binding of LMPTP and other proteins to the SAM domain of the receptor. Development of negative charge on one surface of the SAM domain oligomer could recruit a still unidentified basic protein. Thus, receptor clustering and consequent SAM domain oli-

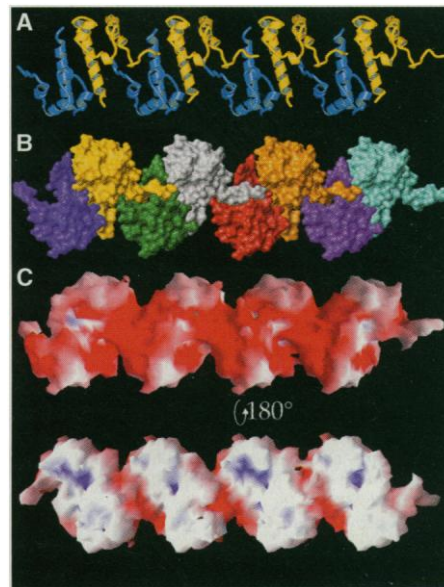


Fig. 3. Model of the SAM domain oligomer. (A) Ribbon diagram. Packing of the monomer with a combination of arm-exchange interfaces and b-region interfaces creates an oligomer. In the ribbon diagram, the S- and L-forms are colored yellow and blue as in Fig. 1. (B) Surface diagram. Each monomer is rendered with a unique color to illustrate the packing at each interface. A 1.4 \AA probe radius was used to calculate the molecular surface area. This figure was made with MOLMOL (33). (C) Electrostatic potential surface of the oligomer. The asymmetric distribution of charge on each face of the oligomer is shown. Red is negative, white is neutral, and blue is positive. The electrostatic surface was contoured between $-10 k_B T/e$ and $+10 k_B T/e$, where k_B is the Boltzmann constant, T is temperature, and e is the electronic charge. This figure was made with GRASP (33).

gomerization would provide a platform for the formation of larger protein complexes.

SAM domain interactions in other proteins are energetically favorable and may therefore mediate the formation of stable complexes in the cell that resemble the polymeric structure described for the EphB2 SAM domain. Indeed, the PcG proteins form large multiprotein complexes. SAM domains from the PcG proteins are relatively promiscuous in their interactions, suggesting that such oligomers could contain a variety of SAM domains. If so, a wide array of binding pockets could be created between SAM domains, multiplying the potential complexity of the surface for specific interactions with other proteins. Though not yet observed, Eph receptors could also form heterogeneous receptor complexes and potentially trigger a wider variety of signaling cascades. It is known that their ligands, the ephrins, can bind to multiple receptor isoforms and could therefore mediate hetero-oligomeric receptor formation (32). Similar combinatorial mechanisms are used by other cell surface receptors (33).

SAM domains are a diverse family of protein modules involved in many biological processes. As a result, their functional roles may vary and alternate oligomerization mechanisms may be used in different contexts. The EphB2-SAM domain structure described here provides a structural foundation for uncovering the functional roles of this important protein interaction module (35).

References and Notes

1. M. Tessier-Lavigne, *Cell* **82**, 345 (1995); H. Hirai, Y. Maru, K. Hagiwara, J. Nishida, F. Takaku, *Science* **238**, 1717 (1987).
2. F. Sakane, S. Imai, M. Kai, I. Wada, H. Kanoh, *J. Biol. Chem.* **271**, 8394 (1996).
3. H. Tu, M. Barr, D. Dong, M. Wigler, *Mol. Cell. Biol.* **17**, 5876 (1997).
4. J. Shultz, C. P. Ponting, K. Hoffman, P. Bork, *Protein Sci.* **6**, 249 (1997).
5. C. P. Ponting, *ibid.* **4**, 1928 (1995).
6. M. Kyba and H. Brock, *Dev. Genet.* **22**, 74 (1998).
7. D. Bornemann, E. Miller, J. Simon, *Development* **122**, 1621 (1996).
8. M. Therrien, A. M. Wong, G. M. Rubin, *Cell* **95**, 343 (1998).
9. T. Pawson, *Nature* **373**, 575 (1995); _____ and J. D. Scott, *Science* **278**, 2075 (1997).
10. C. Jousset *et al.*, *EMBO J.* **16**, 69 (1997); T. Golub, G. Barker, M. Lovett, D. Gilliland, *Cell* **77**, 307 (1994).
11. The SAM domain of the ETS family of transcription factors has been called a pointed domain. Kyba and Brock (6), however, uncovered a clear sequence relation between the pointed domain and the SAM domain. The relation between the pointed domain and the SAM domain is confirmed by comparison of the EphB2 SAM domain and the structure of the pointed domain from the ETS-1 transcription factor [C. M. Slupsky *et al.*, *Proc. Natl. Acad. Sci. U.S.A.* **95**, 12129 (1998)]. The two structures show a common global folding pattern. There are significant differences in the structures, however, particularly at the NH₂-terminus and in the long loop region between the second and the fourth helices of the EphB2-SAM domain.
12. T. Golub *et al.*, *Proc. Natl. Acad. Sci. U.S.A.* **92**, 4917 (1995); M. Carroll, M. Tomasson, G. Barker, T. Golub, D. Gilliland, *ibid.* **93**, 14845 (1996); P. Papadopoulos, S. A. Ridge, C. A. Boucher, C. Stocking, L. M. Wiedemann, *Cancer Res.* **55**, 34 (1995); S. Tosi *et al.*, *Genes Chromosomes Cancer* **21**, 223 (1998).
13. V. Lacronique *et al.*, *Science* **278**, 1309 (1997).
14. A. Peterson *et al.*, *Mol. Cell. Biol.* **17**, 6683 (1997).
15. M. Barr, H. Tu, L. Van Aelst, M. Wigler, *ibid.* **16**, 5597 (1996).
16. C. D. Thanos, C. A. Kim, J. U. Bowie, unpublished results.
17. C. Serra-Pages *et al.*, *EMBO J.* **14**, 2827 (1995).
18. E. Stein *et al.*, *Genes Dev.* **12**, 667 (1998).
19. E. Stein, D. Cerretti, T. Daniel, *J. Biol. Chem.* **271**, 23588 (1996).
20. B. B. Hock *et al.*, *Proc. Natl. Acad. Sci. U.S.A.* **95**, 9779 (1998).
21. H. U. Wang, Z.-F. Chen, D. J. Anderson, *Cell* **93**, 741 (1998); Q. Xu, G. Allous, R. Macdonald, D. Wilkinson, N. Holder, *Nature* **381**, 319 (1996); H.-J. Cheng, M. Nakamoto, A. D. Bergemann, J. G. Flanagan, *Cell* **82**, 371 (1995).
22. W. Hendrickson, J. Horton, D. LeMaster, *EMBO J.* **9**, 1665 (1990); V. Ramakrishnan, <http://snowbird.med.utah.edu/~ramak/madms/segrowth.html>
23. A DNA sequence encoding residues 905 to 981 from EphB2 was amplified by polymerase chain reaction from a human renal microvascular endothelial cell cDNA library and subcloned into a modified pet vector optimized for enhanced expression. The vector-encoded sequence Met-Glu-Lys-Thr-Arg was added to the NH₂-terminus of the SAM domain so that in our numbering scheme, residue 6 corresponds to residue 905 in the full-length receptor. The protein was purified to homogeneity with anion and cation exchange chromatography and gel-filtration chromatography. The protein was crystallized by hanging drop crystallization at 4°C. The drop contained a 1:1 mixture of reservoir buffer and protein at 20 mg/ml. The reservoir contained 100 mM Hepes (pH 7), 10 mM tris, 20 mM dithiothreitol, 30 mM Li₂SO₄, and 26 to 30% Peg 1000.
24. V. Biou and V. Ramakrishnan, *Methods Enzymol.* **276**, 538 (1997).
25. A. T. Brünger, *Nature* **355**, 472 (1992); P. D. Adams, N. S. Pannu, R. J. Read, A. T. Brünger, *Proc. Natl. Acad. Sci. U.S.A.* **94**, 5018 (1997); N. S. Pannu and R. J. Read, *Acta Crystallogr.* **52**, 659 (1996).
26. The conserved residues in the family of SAM domains as defined by Shultz *et al.* (4) are all buried within a monomer, with two exceptions. The first exception is Gly⁵³, which is found in a tight turn between helices 3 and 4. This residue adopts a positive ϕ angle and glycine is probably needed to facilitate the otherwise unfavorable backbone conformation. The second exception is Tyr⁸ on the NH₂-terminal loop. Tyrosine-8 is the key residue in one of the oligomeric interfaces.
27. H. L. De Bondt *et al.*, *Nature* **363**, 595 (1993).
28. J. Janin and F. Rodier, *Proteins Struct. Funct. Genet.* **23**, 580 (1995).
29. D. A. Doyle *et al.*, *Cell* **85**, 1067 (1996).
30. In 31 Eph receptor sequences, Asp⁴⁸ is invariant, position 16 is always a negatively charged residue, position 28 is a negatively charged residue in 30 sequences, and position 47 is a negatively charged residue in 29 sequences.
31. C. D. Thanos, M. Phillips, J. U. Bowie, data not shown.
32. N. W. Gale *et al.*, *Neuron* **17**, 9 (1996).
33. E. Ruoslahti and M. D. Pierschbacher, *Science* **238**, 491 (1987); A. Weiss and J. Schlessinger, *Cell* **94**, 277 (1998).
34. R. Miller, S. M. Gallo, H. G. Khalak, C. M. Weeks, *J. Appl. Crystallogr.* **27**, 613 (1994); Z. Otwinowsky, in *Isomorphous Replacement and Anomalous Scattering, Proceedings of the CCP4 Study Weekend*, W. Wolf, P. R. Evans, A. G. W. Leslie, Eds. (SERC Daresbury Laboratory, Warrington, UK, 1991), pp. 80–86; K. D. Cowtan and P. Main, *Acta Crystallogr. D* **52**, 43 (1996); T. A. Jones, J. Y. Zou, S. W. Cowan, M. Kjeldgaard, *Acta Crystallogr. A* **47**, 110 (1991); A. T. Brünger *et al.*, *Acta Crystallogr. D* **54**, 905 (1998).
35. P. J. Kraulis, *J. Appl. Crystallogr.* **24**, 946 (1991); R. Koradi *et al.*, *J. Mol. Graphics* **14**, 51 (1996); A. Nicholis *et al.*, *Proteins Struct. Funct. Genet.* **11**, 281 (1991).
36. We thank M. Phillips for performing the sedimentation experiments, T. Daniel for clones and helpful discussions, and D. Eisenberg, T. Yeates, D. Cascio, S. Faham, R. Landgraf, F. Pettit, C. Kim, E. Toth, C. Colovos, E. Marcotte, and M. Saper for advice and comments on the manuscript. Supported by an NSF National Young Investigator and a Pew Scholar Award to J.U.B. and an NIH training grant to C.D.T. This work is dedicated to the memory of Marcia Robb Whitt.

13 November 1998; accepted 29 December 1998

Single-Channel Recording of a Store-Operated Ca²⁺ Channel in Jurkat T Lymphocytes

Hubert H. Kerschbaum¹ and Michael D. Cahalan^{2*}

In T lymphocytes, a store-operated calcium ion (Ca²⁺) entry mechanism termed the calcium release-activated Ca²⁺ channel (CRAC channel) underlies the sustained or oscillatory intracellular calcium concentration signal required for interleukin-2 gene expression and cell proliferation. The use of sodium ions as a current carrier enabled single-channel recordings of CRAC channels during activation, inactivation, and blockade of current in the presence of divalent cations. A large conductance of 36 to 40 picosiemens indicates that 100 to 400 CRAC channels are present in T lymphocytes.

Calcium influx is activated by the depletion of calcium ions from intracellular stores in many electrically inexcitable cells (1). In T

lymphocytes, a specific type of store-operated channel, the CRAC channel, supports the intracellular calcium concentration signal that leads to lymphocyte activation (2). CRAC channels are highly selective for calcium ions under physiological conditions (3) and have a tiny single-channel conductance, estimated by fluctuation analysis to be 24 fS in 100 mM extracellular calcium (4). This conductance is too low to be resolved at the single-channel

¹Department of Animal Physiology, Institute of Zoology, University of Salzburg, A-5020 Salzburg, Austria.

²Department of Physiology and Biophysics, University of California, Irvine, CA 92697, USA.

*To whom correspondence should be addressed. E-mail: mcahalan@uci.edu